characterization of brefeldin A-ADP-ribosylated substrate. A novel protein involved in the maintenance of the Golgi structure. *J. Biol. Chem.* **274,** 17705–17710.

Turner, J., and Crossley, M. (1998). Cloning and characterization of mCtBP2, a co-repressor that associates with basic Kruppel-like factor and other mammalian transcriptional regulators. *EMBO J.* **17,** 5129–5140.

Weigert, R., Silletta, M. G., Spanò, S., Turacchio, G., Cericola, C., Colanzi, A., Senatore, S., Mancini, R., Polishchuk, E. V., Salmona, M., Facchiano, F., Burger, K. N., Mironov, A., Luini, A., and Corda, D. (1999). CtBP/BARS induces fission of Golgi membranes by acylating lysophosphatidic acid. *Nature* **402,** 429–433.

Yang, J.-S., Lee, S. Y., Spanò, S., Gad, H., Zhang, L., Bonazzi, M., DeBono, C. A., Branch Moody, D., Barr, F. A., Corda, D., Luini, A., and Hsu, V. W. (2006). BARS participates in the fission of COPI vesicles from Golgi membrane. *EMBO J.*

# [28] *In Vitro* Assays of Arf1 Interaction with GGA Proteins

*By* Hye-Young Yoon, Juan S. Bonifacino, and Paul A. Randazzo

## Abstract

ADP-ribosylation factor 1 (Arf1) is a GTP-binding protein that regulates membrane traffic. This function of Arf1 is, at least in part, mediated by Arf1•GTP binding to coat proteins such as coatomer, clathrin adaptor protein (AP) complexes 1 and 3, and $\gamma$-adaptin homology-Golgi associated Arf-binding (GGA) proteins. Binding to Arf1•GTP recruits these coat proteins to membranes, leading to the formation of transport vesicles. Whereas coatomer and the AP complexes are hetero-oligomers, GGAs are single polypeptide chains. Therefore, working with recombinant GGAs is straightforward compared to the other Arf1 effectors. Consequently, the GGAs have been used as a model for studying Arf1 interactions with effectors and as reagents to determine Arf1•GTP levels in cells. In this chapter, we describe *in vitro* assays for analysis of GGA interaction with Arf1•GTP and for determining intracellular Arf1•GTP levels.

## Introduction

Arfs are members of a family of Ras-like small GTP-binding proteins (Moss and Vaughan, 1998; Randazzo *et al.*, 2000). They are ubiquitously expressed in eukaryotic cells and are highly conserved. The six mammalian


0076-6879/05 $35.00
DOI: 10.1016/S0076-6879(05)04028-0

Arf proteins are grouped into class I (Arf1, 2, and 3), class II (Arf4 and 5), and class III (Arf6) based on sequence homology. Arfs were originally named for their function as cofactors for ADP-ribosylation of heterotrimeric G proteins catalyzed by cholera toxin. Subsequent studies, however, have shown that their main physiologic function is regulation of membrane traffic.

Arf regulation of membrane traffic depends on their interaction with a subset of coat proteins that are critical components of the membrane traffic machinery (Bonifacino and Glick, 2004; Bonifacino and Lippincott-Schwartz, 2003; Kirchhausen, 2002; Owen *et al*., 2004; Robinson and Bonifacino, 2001). Among the coat proteins that interact with Arf are a heteroheptameric complex named coatomer, which polymerizes to form COPI coats, and the heterotetrameric adaptors AP-1 and AP-3, which are incorporated into clathrin coats. The structurally related non-clathrin adaptor AP-4 also interacts with Arf, as do the single polypeptide GGA clathrin adaptors. Although all Arfs bind to these proteins to some extent, class I Arfs such as Arf1 and Arf3 are the most active for coat protein recruitment. Therefore, we focus our discussion and methods on Arf1. In the current paradigm (Bonifacino and Glick, 2004; Bonifacino and Lippincott-Schwartz, 2003; Nie *et al*., 2003; Randazzo *et al*., 2000; Spang, 2002; Springer *et al*., 1999). Arf1•GDP exchanges nucleotide to form Arf1•GTP. Arf1•GTP binds tightly to membranes via its myristoylated N-terminal $\alpha$-helix and to the protomer form of the coat proteins via its switch 1 and switch 2 regions. This results in recruitment of the coat protomers to the cytosolic surface of membranes. The coat protomers can then bind to and trap transmembrane cargo molecules, as well as polymerize into a vesicle coat that drives deformation of the membrane and budding of a transport vesicle.

Three GGA proteins exist in humans (i.e., GGA1, GGA2, and GGA3) and 1–3 in most other eukaryotes (Bonifacino, 2004; Ghosh and Kornfeld, 2004). The GGAs are comprised of four domains, from N- to C-terminus, VHS, GAT, hinge, and GAE (Bonifacino, 2004; Boman *et al*., 2000; Dell'Angelica *et al*., 2000; Hirst *et al*., 2000; Nakayama and Wakatsuki, 2003). The VHS domain of the mammalian GGAs binds to acidic cluster dileucine or DXXLL sorting motifs in intracellular transport receptors such as the cation-independent and cation-dependent mannose 6-phosphate receptors (Ghosh *et al*., 2003; Nielsen *et al*., 2001; Puertollano *et al*., 2001a; Takatsu *et al*., 2001). The GAT domain binds to Arf1•GTP, Rabaptin-5, ubiquitin, and TSG101 (Bilodeau *et al*., 2004; Dell'Angelica *et al*., 2000; Mattera *et al*., 2003, 2004; Puertollano *et al*., 2001b; Scott *et al*., 2004; Shiba *et al*., 2004). The unstructured hinge region binds to clathrin (Puertollano *et al*., 2001b). The GAE domain interacts with accessory

proteins including γ-synergin, p56, Rabaptin-5, enthoprotin, and aftiphilin (Lui *et al.*, 2003; Mattera *et al.*, 2003).

Given that GGAs comprise a single modular polypeptide, expression of the recombinant domains has been relatively straightforward. The domains expressed in bacteria are soluble and have the same activities, including cargo, Arf1, clathrin, and accessory protein binding, as in the full-length proteins expressed in mammalian cells. Because of these properties, GGA has been extensively studied with significant progress in understanding structure–function relationships. The crystal structures of the VHS (Misra *et al.*, 2001; Zhu *et al.*, 2003a), GAT (Collins *et al.*, 2003b; Miller *et al.*, 2003; Zhai *et al.*, 2003; Zhu *et al.*, 2003b, 2004) and GAE (Collins *et al.*, 2003a; Miller *et al.*, 2003; Nogi *et al.*, 2002) domains, alone or in complexes with their binding partners, have been determined. The domain that interacts with Arf1, GAT, is an elongated, all α-helical fold that forms two subdomains. There is an N-terminal "hook" subdomain consisting of a short α-helix folding with the N-terminal portion of a longer α-helical segment, with a loop separating the two α-helices. This structure interacts with the switch 1 and switch 2 regions (parts of Arf that are sensitive to nucleotide) of Arf1•GTP. The C-terminal subdomain consists of a three α-helix bundle and is involved in binding ubiquitin, Rabaptin 5, and TSG101. The putative binding sites are far apart so that both binding sites can be occupied simultaneously.

Because of their simpler structure, the GGAs have been used as a model for studying the interactions of Arf1 with effectors. Much work has been done using yeast two-hybrid and mutagenesis (see for example Kuai and Kahn, 2000; Kuai *et al.*, 2000; Puertollano *et al.*, 2001b). Using *in vitro* assays, GGA binding to Arf1 has been further characterized in respects that could not be done by two-hybrid assays. In addition to quantifying the relative effects of switch 1 and switch 2 mutants, the *in vitro* assays have allowed examination of the effects of cargo, acid phospholipids, and domains adjacent to the GAT domain, on Arf1-GGA interaction (Hirsch *et al.*, 2003; Jacques *et al.*, 2002). Here, we describe several approaches we have used for studying GGA interactions with Arf1 in solution, and a method using GGA for the determination of Arf1•GTP levels *in vivo*.

## Methods

### *Preparation of Recombinant GGA Domains*

For the assays described in this chapter, constructs comprised of the GAT domain of GGA proteins, and additional domains as necessary for the question being addressed, are expressed in bacteria. The proteins are

fused to tags to aid in purification. GST-fusion proteins work well for all the methods described (Dell'Angelica *et al.*, 2000; Puertollano *et al.*, 2001b). GST-VHSGAT$_{GGA3}$ (residues 1–313 of GGA3) and GST-GAT$_{GGA3}$ (residues 147–313) were generated using the plasmid pGEX-5X-1 (Amersham Biosciences, Piscataway, NJ). The open reading frames were amplified with *Eco*RI and *Not*I restriction sites at the 5′ and 3′ ends and were subcloned into pGEX-5X-1 by standard DNA recombinant procedures. His$_{10}$-tagged proteins are also useful and have the added benefit that they do not dimerize as readily. His$_{10}$-VHSGATGGA1 (residues 1–315 of GGA1) and His$_{10}$-GAT$_{GGA1}$ (residues 148–315 of GGA1) were generated using the plasmid pET19 (Novagen, Madison, WI) (Hirsch *et al.*, 2003; Jacques *et al.*, 2002; Puertollano *et al.*, 2001b). The open reading frame was amplified by PCR incorporating *Nde*I and *Bam*HI restriction sites that were used to subclone into the plasmid.

GST-fusion proteins and His$_{10}$-tagged proteins are expressed in *E. coli* BL21(DE3) bacteria using the same protocol. Transformed bacteria are selected with ampicillin. A single colony is grown in 200 ml Luria-Bertani (LB) medium containing 100 $\mu$g ampicillin per ml until $OD_{600} = 0.6$ at 37°. The bacteria are cooled to 4° and refrigerated overnight. The next day, the bacteria are collected by centrifugation and resuspended in 1–21 of LB medium with 100 $\mu$g/ml ampicillin. The culture is maintained at 37° until it reaches $OD_{600} = 0.6$ and then isopropyl thio-$\beta$-D-galactylpyranoside (IPTG) is added to a final concentration of 1 m*M*. After IPTG induction, the bacteria are grown for an additional 3 h at 37° and then harvested by centrifugation at 1500–2500*g* for 20 min at 4°.

To purify the bacterially expressed proteins, the cell pellets from 250–500 ml of cell culture are suspended in 10 ml of phosphate-buffered saline (PBS) containing a Complete® protease inhibitor tablet (Roche, Indianapolis, IN) and 0.1% (w/v) Triton X-100 and lysed with a French press operated at 12,000 psi (double the volume of PBS if using 1–2l of cell culture). For the His10-tagged protein, an EDTA-free protease inhibitor cocktail is used (also available from Roche). The soluble material is clarified by centrifugation at 100,000*g* for 60 min at 4°. Both GST-fusion proteins and His$_{10}$-tagged proteins can be purified by batch adsorption to and elution from glutathione-Sepharose 4 B (Amersham Biosciences) or a metal-chelating resin (e.g., Talon® from Clontech or Ni-NTA from Qiagen, Valencia, CA), respectively, using methods described by the manufacturer of the resin. We prefer to use columns. For GST-fusion proteins, the clarified cell lysate is loaded onto 300 $\mu$l of glutathione-Sepharose 4 B packed in a Poly-Prep chromatography column (Bio-Rad) equilibrated with PBS. The column is washed with 1–2 ml of ice-cold PBS and proteins eluted with 10 m*M* glutathione, 50 m*M* Tris-HCl, pH 8.0, and 100 m*M*

NaCl in 5 fractions of 300 $\mu$l. 5 $\mu$l samples of the 5 fractions are analyzed by SDS-PAGE and the 1 or 2 fractions that together contain more than 90% of the proteins are taken. For His10-tagged proteins, we use a HisTrap™ column (Amersham Biosciences). The His10-tagged protein is adsorbed to the column equilibrated with 20 m*M* Tris-HCl, pH 8.0, 500 m*M* NaCl, and 10 m*M* imidazole, pH 7.0. The protein is then eluted with a gradient from 10 to 500 m*M* imidazole, pH 7.0, in 500 m*M* NaCl. Both GST-fusion and His10-tagged proteins are desalted by using a PD-10 column (Amersham Biosciences), equilibrated, and run with ice-cold PBS or 20 m*M* Tris-HCl, pH 7.5, 100 m*M* NaCl, and 1 m*M* dithiothreitol (DTT). The 0.5–1.5 ml sample is applied to a PD-10 column and 1 ml fractions are collected. The 1 or 2 fractions containing greater than 90% of the protein, determined using the Bio-Rad dye-binding protein assay, are pooled.

### *Preparation of Other Recombinant Proteins*

The preparation of $His_{10}$[325-724]ASAP1 is described in Randazzo *et al.* (2000). The preparation of myristoylated Arf1 is described in Chapter 16 of this volume (Preparation of Myristoylated Arf1 and Arf6). The preparation of non-myristoylated Arf1, is described in Randazzo *et al.* (1992). The same method is used for the purification of [L8K]Arf1, which is described in Yoon *et al*. (2004).

### *Loading Arf1 with [$^{35}$S]GTP$\gamma$S and [$\alpha^{32}$P]GTP*

For the methods we describe here, Arf1•GTP is used at a concentration that is much lower than the measured dissociation constant for the GGA•Arf1•GTP complex ($K_d$) or the Michaelis constant (i.e., the concentration of Arf1•GTP that gives half maximal velocity of GAP-induced GTP hydrolysis, $K_m$) for Arf GAP. Under this condition, the equations that are derived for the analysis of the data are simple hyperbolics rather than quadratics (see following).

For two assays, Arf1•[$^{35}$S]GTP$\gamma$S is prepared by incubating 1–5 $\mu$*M* Arf1 with 15 $\mu$*M* [$^{35}$S]GTP$\gamma$S (specific activity $\approx$ 50,000 cpm/pmol) in 20 m*M* Tris-HCl, pH 7.5, 100 m*M* NaCl, 1 m*M* EDTA, 0.5 m*M* $MgCl_2$, 1 m*M* DTT, and 0.1% (w/v) Triton X-100 for 1 h at 30°. [$\alpha^{32}$P]GTP•Arf1 is prepared in a similar way. However, in this case, steps are taken to ensure that contaminating nucleotidases (very difficult to completely remove from Arf1) do not significantly degrade GTP before it is able to bind to Arf1. Two approaches have worked for us. One way is to incubate 1–5 $\mu$*M* Arf1 with 10 $\mu$*M* [$\alpha^{32}$P]GTP (specific activity $\approx$ 50,000 cpm/pmol) in 20 m*M* Tris-HCl, pH 7.5, 1 m*M* EDTA, 0.5 m*M* $MgCl_2$, 1–2 m*M* ATP, 1 m*M* DTT, and 0.1% (w/v) Triton X-100 for 30–60 min at 30°. High concentrations of

ATP inhibit nonspecific nucleotidases. Another way to prepare [$\alpha^{32}$P]GTP•Arf1 for the GAP assay is to incubate Arf1 with 25 m*M* HEPES, pH 7.4, 100 m*M* NaCl, 3.5 m*M* $MgCl_2$, 1 m*M* EDTA, 1 m*M* ATP, 1 $\mu M$ [$\alpha^{32}$P]GTP (specific activity = 50,000–250,000 cpm/pmol), 25 m*M* KCl, 1.25 U/ml pyruvate kinase, and 3 m*M* phosphoenolpyruvate. This buffer contains a GTP regenerating system. If using Arf1 that has not been myristoylated, include 0.1% (w/v) Triton X-100. For myristoylated Arf1, use either micelles of 3 m*M* dimyristoylphosphatidylcholine and 0.1% cholate, pH 7.4 or use vesicles prepared by extrusion or sonication (see Chapter 15 of this volume, Assay and Properties of the Arf GAPs AGAP1, ASAP1, and ArfGAP1).

### *Three Assays for GGA•Arf1 Interactions*

*Direct Determination of Binding.* With a $K_d$ of greater than 200 n*M* for Arf1•GTP•GGA interactions, conventional pull-down assays are not quantitative due to rapid dissociation during the washes. Nonetheless, these assays are useful for establishing that there is a specific interaction between GGA and Arf1•GTP. We show an example of data from a direct binding assay in Fig. 1. In a typical experiment, 10 $\mu$g of GST or GST-VHSGATGGA3 are added to 450 $\mu$l of a cell lysate, for example, bovine brain lysate, containing 20 m*M* Tris-HCl, pH 8.0, 100 m*M* NaCl, 0.1% (w/v)

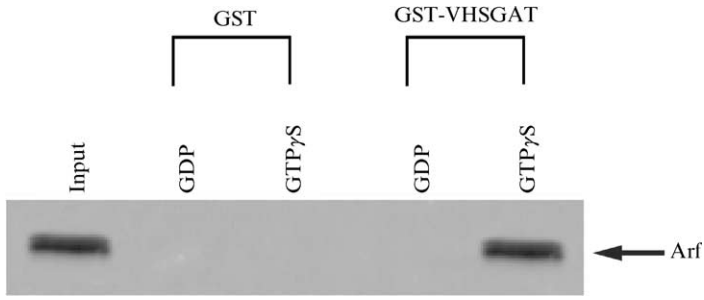


FIG. 1. Pull-down assay for Arf•GTP association with GST-VHSGAT$_{GGA3}$. GSTVHSGAT$_{GGA3}$ (10 $\mu$g) or GST was incubated with a bovine brain lysate containing 0.1% (w/v) Triton X-100 and 100 $\mu M$ GDP or GTP$\gamma$S for 30 min at 30° and then chilled to 4° for 5 min. GST and GST-VHSGAT$_{GGA3}$ were precipitated with glutathione-agarose. The precipitate was washed 3 times with ice-cold PBS containing 0.1% (w/v) Triton X100 and the associated proteins were fractionated by SDS-PAGE and transferred to nitrocellulose. Arf was detected by immunoblotting with a mouse monoclonal antibody 1D9 from Affinity BioReagents used at a dilution of 1:500, a goat anti-mouse IgG-HRP conjugate (Bio-Rad) used at a dilution of 1:10,000 and ECL plus Western blotting detection reagent (Amersham Biosciences).

Triton X-100, and 20 $\mu M$ GTP$\gamma$S. The mixture is incubated at 30° for 30–60 min and then chilled. Glutathione-agarose beads, 25 $\mu$l, are added and the mixture is incubated an additional 30 min at 4°. The beads are collected by a brief centrifugation (13,000$g$ in a table-top refrigerated microcentrifuge for 30 sec) and washed 3 times with ice-cold PBS containing 0.1% (w/v) Triton X-100. Arf1 can be detected in the pellet by immunoblotting using a commercially available antibody, such as monoclonal mouse anti-Arf (1D9) from Affinity Bioreagents (Golden, CO) (Fig. 1). This approach can be exploited for measuring Arf1•GTP levels *in vivo* as described in the following.

For quantitative analysis, we use a method that is a variation of dialysis binding assays (Jacques *et al.*, 2002). In this case, instead of using a dialysis membrane to separate two volumes, one with the "receptor" (in this case, a GGA construct such as GST-VHSGAT, abbreviated "GGA" in the equations that follow) and one excluding the "receptor," we generate two de facto compartments by immobilizing GST-GGA protein on glutathione-agarose beads. After a brief incubation with Arf1•GTP$\gamma$S, two volumes are generated by a brief centrifugation, maintaining the temperature of the assay, and separated into two scintillation vials by pipetting. The volume with the beads contains Arf1•GTP$\gamma$S•GGA and free Arf1•GTP$\gamma$S, whereas the volume excluding the beads contains only free Arf1•GTP$\gamma$S. Assuming the volume containing the beads is 20% of the total reaction volume, then,

$$(\text{Arf1} \bullet \text{GTP}\gamma\text{S})_{pellot} = 0.2(\text{Arf1} \bullet \text{GTP}\gamma\text{S})_{total} + 0.8\frac{B_{max}[\text{GGA}]}{[\text{GGA}] + K_d} \quad (1)$$

where $K_d$ is the Arf•GGA dissociation constant (also abbreviated $K_{GGA}$) and $B_{max}$ is the maximum binding. To perform this assay, Arf1 is loaded with [$^{35}$S]GTP$\gamma$S in one reaction. Varying amounts of a GGA fragment fused to GST (e.g., GST-VHSGAT) are immobilized on glutathione-agarose beads such that 10 $\mu$l of the beads added to a 50–100 $\mu$l reaction will yield a GGA protein concentration of between 0 and 5 $\mu M$. Arf1•GTP$\gamma$S is then added to the GGA protein immobilized on 10 $\mu$l of beads in a reaction that contains 20 m$M$ Tris-HCl, pH 7.5, 100 m$M$ NaCl, 1 m$M$ $MgCl_2$, 1 m$M$ DTT, 0.1% (w/v) Triton X-100, and other additions such as phospholipids in a total volume of 100 $\mu$l. The mixture is incubated for 5–10 min at 30°. The beads are separated from the bulk solution by a 5–10 sec centrifugation at 13,000$g$ in a tabletop microcentrifuge. [$^{35}$S]GTP$\gamma$S in 80 $\mu$l of the supernatant and in the 20 $\mu$l containing the beads are quantified by scintillation spectrometry. The fraction of [$^{35}$S]GTP$\gamma$S in the pellet is plotted against the concentration of GGA protein in the pellet and the data are fit to Eq. (1), using a nonlinear least squares algorithm, to

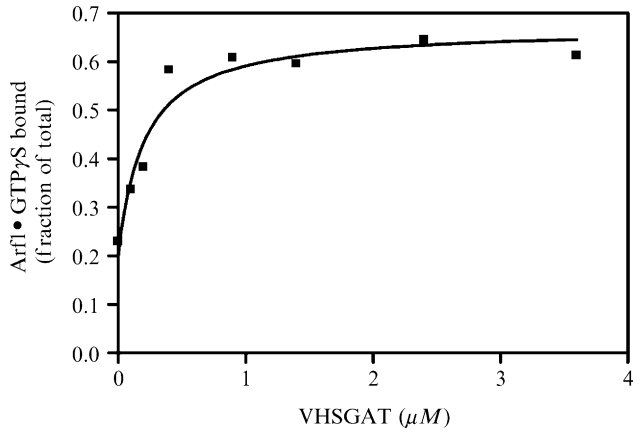


FIG. 2. Results from a direct binding assay. The fraction of total Arf1•GTPγS that was associated with GST-VHSGAT$_{GGA3}$ immobilized on glutathione beads is plotted against the concentration of GST-VHSGAT$_{GGA3}$ in the assay. The data were fit to Eq. (1).

determine the $K_d$. For fitting the data, we use a program called GraphPad Prism (GraphPad Software, San Diego, CA). Other scientific graphics programs also have suitable curve fitting capabilities. The data are entered with the amount of Arf1•GTPγs in the pellet as "y" and the concentration of GGA as "x." The process of analyzing the data is menu driven and also well explained in the software's documentation. Example data are shown in Fig. 2.

We have also used this approach for characterizing the binding of Arf1•GTP to the Arf GAP, AGAP1, in which case the determined $K_d$ fit well with that calculated using other approaches. This approach has an advantage over surface plasmon resonance or isothermal titrating calorimetry in that (i) it does not require chemical concentrations of Arf1•GTP, which are sometimes difficult to achieve and (ii) the results are not skewed by differences in efficiency of GTP binding that might occur when using Arf1 mutants.

### *Binding Determined by Inhibition of Arf GAP Activity*

GGA proteins bind Arf1 through the switch 1 and switch 2, which overlap the GAP binding site. Therefore, GGA binding to Arf1•GTP inhibits GAP activity (see Fig. 3). If the concentrations of both Arf1•GTP and Arf GAP (in this case, we use ASAP1) are less than the $K_m$ for the GAP, and the concentration of Arf1•GTP is significantly less than

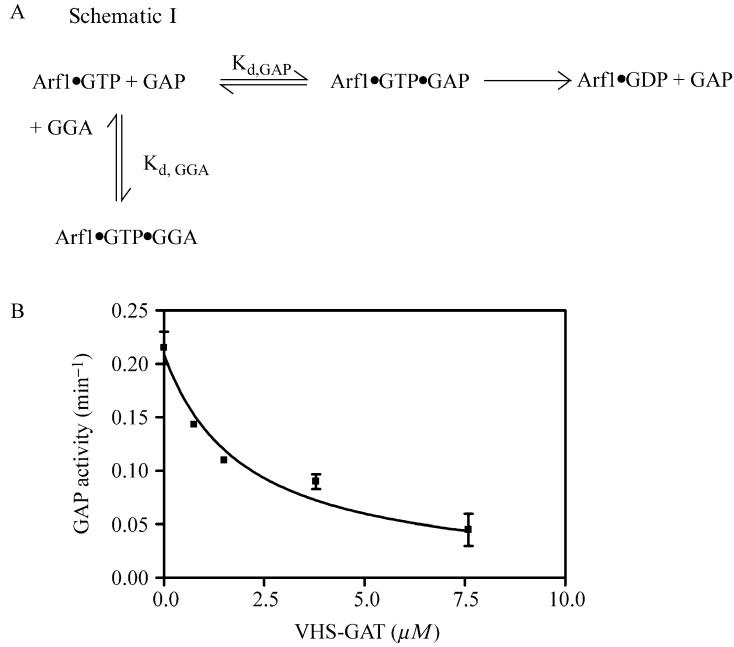


FIG. 3. Determination of GGA-Arf binding by inhibition of GAP activity. (A) Schematic of reaction. (B) Data from example experiment. GST-VHSGAT$_{GGA3}$, Arf1, and [325–724] ASAP1 were used as described in the text. Data were fit to Eq. (2) and GAP activity was calculated using Eq. (3).

the $K_d$ for the GGA•Arf1•GTP complex, then we can derive Eq. (2) describing the relationship of GAP activity and GGA concentration. In the equation $V_{obs}$ is the rate of GTP hydrolysis observed in the presence of a given concentration of GGA and $V_{noGGA}$ is the rate in the absence of GGA. The identical equation is obtained under equilibrium and steady state assumptions. Based on this equation, the concentration of GGA that gives half maximal inhibition is the $K_d$ for the GGA•Arf1•GTP complex (Hirsch *et al.*, 2003; Jacques *et al.*, 2002; Puertollano *et al.*, 2001b).

$$V_{obs} = \frac{V_{noGGA}}{1 + \frac{GGA}{K_d}} \tag{2}$$

For this assay, we use ASAP1, a robust Arf GAP with a turnover number ($k_{cat}$) of approximately 30/sec, and a $K_m$ of approximately 5 $\mu M$ (Che *et al.*, 2005). With these parameters, nanomolar concentrations of Arf1 and the GAP can be used with an excellent signal to noise ratio for a

3–5 min assay. Arf1 is loaded with [$\alpha^{32}$P]GTP using one of the two methods described above. In separate tubes kept at 4°, add between 0.2 and 1 n*M* [325–724]ASAP1[1] in 20 m*M* HEPES, pH 7.4, 100 m*M* NaCl, 2 m*M* $MgCl_2$, 1 m*M* GTP, 1 m*M* DTT, 360 $\mu M$ phosphatidic acid, and 90 $\mu M$ phosphatidylinositol 4, 5bisphosphate in 0.1% Triton X-100 and varying amounts of the GGA being examined in a total volume of 22.5 $\mu$l. Initiate the GAP reaction by the addition of 2.5 $\mu$l of the mixture containing Arf1•GTP and simultaneously shifting the reaction mixture to 30°. Always, as described in Chapter 15, Assay and Properties of the Arf GAPs AGAP1, ASAP1, and Arf GAP1), include no GAP control to correct for GDP that binds to Arf1 during loading. The reaction is stopped after 3–5 min by dilution into 2 ml of ice-cold 20 m*M* Tris-HCl, pH 8.0, 100 m*M* NaCl, 10 m*M* $MgCl_2$, 1 m*M* DTT. Arf1 is then trapped on nitrocellulose filters. Nucleotide is eluted from the filters using 2 *M* formic acid and a sample of this eluate is separated on a PEI (polyethylenimine)-cellulose TLC plate developed in 1 *M* CHOOH: 1 *M* LiCl. To extend the useful range of the assay, we use a mathematical transform of the data, Equation (3) in which *V* is the velocity (expressed as a first order rate constant), $(Arf1 \bullet GTP)_0$ is the concentration of Arf1•GTP at time 0 (or in the blank), and $(Arf1 \bullet GTP)$ is the concentration of Arf1•GTP at time t in the presence of GAP, as described in Randazzo *et al.* (2001). Further details of this assay are given in Chapter 15 (Assay and Properties of the Arf GAPs AGAP1, ASAP1, and Arf GAP1) of this volume and Randazzo *et al.* (2001).

$$V = \frac{\ln \dfrac{(Arf1 \bullet GTP)_0}{(Arf1 \bullet GTP)}}{t} \tag{3}$$

A sample set of data is shown in Fig. 3B. We use a nonlinear least squares algorithm to fit the data to Eq. (2). The $K_d$ determined is nearly identical to the value obtained by other methods (Jacques *et al.*, 2002).

One disadvantage of this approach is that it is difficult to determine the role of phospholipids because the Arf GAP interaction with Arf1 is also dependent on phospholipids. However, the GAP does not have to be under optimal conditions: simply add more GAP if conditions are less than optimal. Also, other GAPs can be used that do not have as restrictive phospholipids requirements. For instance, Arf GAP1, which does not require phosphatidylinositol 4, 5-bisphosphate, also appears to bind a site on Arf1 that overlaps the binding site for GGA (Jacques *et al.*, 2002) and, therefore, can be used in the assay.

[1] When diluting a highly purified GAP to nanomolar concentrations, the protein is stabilized by including a carrier protein such as bovine serum albumin at a concentration of 100 $\mu$g/ml.

*Binding Determined by Slowing GTPγS Dissociation*

This method is based on an assay developed by Herrmann *et al.* (1995) for the determination of binding affinities of Ras effectors for Ras•GTP. Arf1•GTP and Arf1•GTPγS dissociate at a rate determined by phospholipids, $Mg^{2+}$ concentration and, as illustrated in Fig. 4, associated proteins. Effectors like GGA slow the dissociation rate. We can measure the dissociation rate by first loading Arf1 with a [$^{35}$S]GTPγS of high specific activity and then incubating the Arf1•[$^{35}$S]GTPγS in a reaction mixture containing a high concentration of GTPγS or GDP. As the [$^{35}$S]GTPγS dissociates, the unlabeled nucleotide competes for rebinding. The dissociation rate can be measured as the rate of loss of protein-associated $^{35}$S. The dissociation rate in the absence of effector is $k_{-1}$ and in the presence of effector is $k_{-2}$. The total dissociation rate is

$$-d(\text{Arf1} \bullet \text{GTP}\gamma\text{S})/_{dt} = k_{-1}[\text{Arf1} \bullet \text{GTP}\gamma\text{S}] + k_{-2}[\text{GGA} \bullet \text{Arf1} \bullet \text{GTP}\gamma\text{S}] \tag{4}$$

If $k_{-2} \ll k_{-1}$, this reduces to

$$-d(\text{Arf1} \bullet GTP\gamma S)/_{dt} = k_{-1}[\text{Arf1} \bullet GTP\gamma S] \tag{5}$$

We assume that Arf1 • GTPγS $< K_d$ for the GGA • Arf1 • GTP complex. Under this condition, Arf1•GTPγS that is not bound to GGA is

$$[\text{Arf1} \bullet \text{GTP}\gamma\text{S}] = \frac{[\text{Arf1} \bullet \text{GTP}\gamma\text{S}]_{total} K_d}{[\text{GGA}] + K_d} \tag{6}$$

substituting Eq. (6) into (5) gives

$$-d(\text{Arf1} \bullet \text{GTP}\gamma\text{S})/_{dt} = \frac{k_{-1}}{1 + \dfrac{[\text{GGA}]}{K_d}} [\text{Arf1} \bullet \text{GTP}\gamma\text{S}]_{total} \tag{7}$$

From this expression, the observed dissociation rate at a given concentration of GGA fragment, the $k_{obs}$, is related to the $k_{-1}$ as described by Eq. (8).

$$k_{obs} = \frac{k_{-1}}{1 + \dfrac{[\text{GGA}]}{K_d}} \tag{8}$$

The concentration of GGA that slows dissociation by 50%, the $K_d$, can be determined from a plot kobs against the concentration of GGA.

To be consistent with our assumptions for the derivation, we use a low concentration of Arf1•[$^{35}$S]GTPγS, prepared as described above. This assay benefits from using Arf1 that is not myristoylated because the

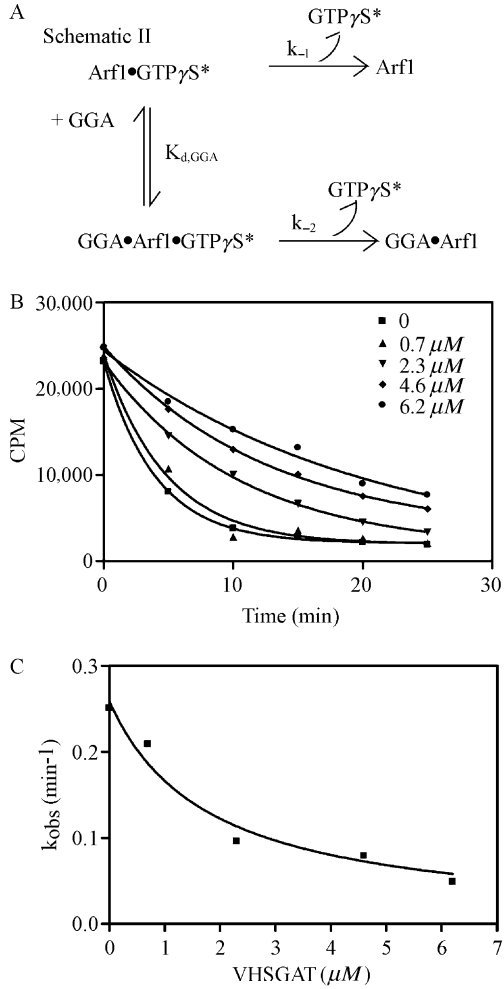


FIG. 4. Inhibition of GTPγS dissociation of Arf1 used in assay for GGA binding to Arf1. (A) Schematic of reactions. (B) Effect of GGA on GTPγS dissociation from Arf1. Nonmyristoylated Arf1•[$^{35}$S]GTPγS was incubated with the indicated amount of GST-$VHSGAT_{GGA3}$. After the indicated period of time, samples were removed and protein-bound [$^{35}$S]GTPγS was determined by filter binding followed by scintillation spectrometry. (C) Plot for determining $K_{d,GGA3}$. The dissociation data, presented in Fig. 4B, were fit to single exponential decay equation (if examine dissociation over linear range, use linear least squares fitting) to determine the dissociation rate. The observed dissociation rates were plotted against the concentration of GGA3 and fit to Eq. (8) to determine the $K_d$.

dissociation rates in the presence of lipid are greater and easier to measure than those for myristoylated Arf1. $Mg^{2+}$ is buffered to approximately 1 $\mu M$ to maximize uncatalyzed dissociation of the Arf1•GTP$\gamma$S complex. The reaction mixture contains 20 m$M$ Tris-HCl, pH 7.5, 100 m$M$ NaCl, 0.5 m$M$ $MgCl_2$, 1 m$M$ EDTA, 0.1% (w/v) Triton X-100, and the GGA protein fragment, for example, VHSGAT, as well as any other additions such as phospholipids in a total volume of 100 $\mu$l. Samples of the reaction are removed at 6–9 time points ranging from 0 to 60 min and quenched by dilution into ice-cold 10 m$M$ Tris-HCl, pH 8.0, 100 m$M$ NaCl, 10 m$M$ $MgCl_2$, and 1 m$M$ DTT. Protein-bound nucleotide is trapped on nitrocellulose filter disks. Scintillation spectrometry is used to quantify $^{35}S$. The progress curves are fit to a single exponential decay equation ($cpm = cpm_0 \cdot e^{-k_{obs} \cdot t}$, e.g., in Fig. 4B, all curves can be fit to this equation) or a line if dissociation is less than 15%) to determine $k_{obs}$. This estimated value of $k_{obs}$ is then plotted against GGA concentration (Fig. 4C) and fit to Eq. (8) using a scientific graphics program to determine the affinity.

One drawback of this method is that it is dependent on the dissociation rates for the Arf1•GTP$\gamma$S complex. Some mutants of Arf1, such as $\Delta$17Arf1, do not have a rapid GTP dissociation rate so signal to noise may be problematic. On the other hand, this method has worked for many switch 1 and switch 2 mutants of Arf1 and is also useful for comparing different proteins derived from GGA. We expect that it will be useful for other Arf effectors but have not yet tested them.

### *Use of GGA for Determining Cellular Levels of Arf1•GTP*

GGA binds Arf1•GTP in preference to Arf1•GDP. This difference in binding has been exploited in an assay to measure intracellular Arf•GTP levels (Santy and Casanova, 2001). The rationale is identical to that for assays developed for Ras (deRooij and Bos, 1997; Franke *et al*., 1997) and Rho (Sander *et al*., 1998) family proteins. Because the presence of the VHS domain of GGA3 improves the affinity of the GAT domain for Arf1 • GTP, we use a fusion protein of GST-$VHSGAT_{GGA3}$ expressed and purified as described previously. This interaction is low affinity; therefore, temperature control is critical. In a typical experiment, cells grown on 35 mm well plates are transfected with expression vectors for Arf1-HA or mutants and any other proteins of interest, such as GAPs or GEFs. After 18–24 h, cells are lysed in 0.5 ml of 50 m$M$ Tris-HCl, pH 7.5, 100 m$M$ NaCl, 2 m$M$ $MgCl_2$, 1% (w/v) Triton X-100, and protease inhibitors at 4°. The lysates are cleared by addition of 20 $\mu$l of Sepharose CL-4B beads, mixing and separating the beads from the lysate by centrifugation at 16,000$g$ for 20 sec at 4°. Fifty $\mu$g of GST-$VHSGAT_{GGA3}$ immobilized on 20 $\mu$l of glutathione-Sepharose

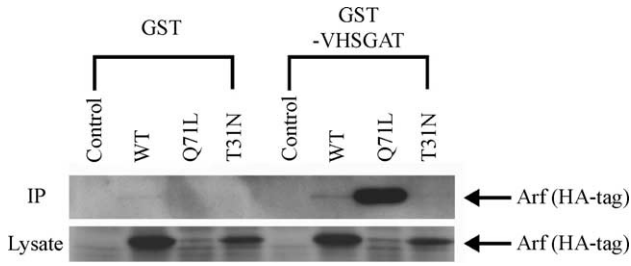


FIG. 5. Use of GST-VHSGAT$_{GGA3}$ as a reagent for determining Arf1•GTP levels *in vivo*. HEK 293 cells were transfected with plasmids directing expression of epitope tagged Arf1, [T31N]Arf1 or [Q71L]Arf1. Eighteen hours later, the cells were lysed. The lysates were incubated with either GST or GST-VHSGAT$_{GGA3}$ and Arf1 associating with GST-VHSGAT$_{GGA3}$ was determined as described in the text. As anticipated, the constitutively active mutant of Arf1, [Q71L], gave a greater signal than wild type protein whereas no signal was detected with the dominant negative protein.

CL-4B beads are added to the cleared lysates and the mixture is incubated at 4° for 1 h. The beads are collected by a brief centrifugation (30 sec at 13,000*g* in a microcentrifuge).

The beads are washed three times with 50 m*M* Tris-HCl, pH 7.5, 100 m*M* NaCl, 2 m*M* $MgCl_2$, and 1% (w/v) Triton X-100 at 4°. To analyze the bound proteins, 60 $\mu$l sample buffer is added to the beads and the mixture is heated at 95° for 5 min. The beads are removed by centrifugation and samples of the supernatant are fractionated by SDSPAGE. Proteins are eluted from the beads by boiling in SDS-PAGE sample buffer, electrophoresed on a 15% SDS-PAGE gel, and transferred to an Immobilon P membrane (Milipore, Bedford, MA). The blot is incubated sequentially with monoclonal mouse anti-HA antibody (Roche, Indianapolis, IN) (1:3000) and with goat anti-mouse IgG-HRP conjugate (1:10,000, Bio-Rad, Hercules, CA). The IgG HRP conjugate is detected using ECL plus Western blotting reagent (Amersham Biosciences) (Fig. 5).

This method is reasonably robust when assaying Arf1 and Arf5. Our laboratory and others following the outlined protocol have obtained interpretable data with both Arf isoforms. Assay of Arf6 appears to be more variable. This may be related to cell differences as well as the solubility properties and stability of Arf6 relative to Arf1.

## References

Bilodeau, P. S., Winistorfer, S. C., Allaman, M. M., Surendhran, K., Kearney, W. R., Robertson, A. D., and Piper, R. C. (2004). The GAT domains of clathrin-associated GGA proteins have two ubiquitin binding motifs. *J. Biol. Chem.* **279,** 54808–54816.

Boman, A. L., Zhang, C. J., Zhu, X. J., and Kahn, R. A. (2000). A family of ADP-ribosylation factor effectors that can alter membrane transport through the *trans*-Golgi. *Mol. Biol. Cell* **11,** 1241–1255.

Bonifacino, J. S. (2004). The GGA proteins: Adaptors on the move. *Nat. Rev. Mol. Cell Biol.* **5,** 23–32.

Bonifacino, J. S., and Glick, B. S. (2004). The mechanisms of vesicle budding and fusion. *Cell* **116,** 153–166.

Bonifacino, J. S., and Lippincott-Schwartz, J. (2003). Opinion – coat proteins: Shaping membrane transport. *Nat. Rev. Mol. Cell Biol.* **4,** 409–414.

Che, M. M., Boja, E. S., Yoon, H.-Y., Gruschus, J., Jaffe, H., Stauffer, S., Schuck, P., Fales, H. M., and Randazzo, P. A. (2005). Regulation of ASAP1 by phospholipids is dependent on the interface between the PH and Arf GAP domains. *Cell. Signal.* **17,** 1276–1288.

Collins, B. M., Praefcke, G. J. K., Robinson, M. S., and Owen, D. J. (2003a). Structural basis for binding of accessory proteins by the appendage domain of GGAs. *Nat. Struct. Biol.* **10,** 607–613.

Collins, B. M., Watson, P. J., and Owen, D. J. (2003b). The structure of the GGA1-GAT domain reveals the molecular basis for ARF binding and membrane association of GGAs. *Dev. Cell* **4,** 321–332.

Dell'Angelica, E. C., Puertollano, R., Mullins, C., Aguilar, R. C., Vargas, J. D., Hartnell, L. M., and Bonifacino, J. S. (2000). GGAs: A family of ADP ribosylation factor-binding proteins related to adaptors and associated with the Golgi complex. *J. Cell Biol.* **149,** 81–93.

deRooij, J., and Bos, J. L. (1997). Minimal Ras-binding domain of Raf1 can be used as an activation-specific probe for Ras. *Oncogene* **14,** 623–625.

Franke, B., Akkerman, J. W. N., and Bos, J. L. (1997). Rapid $Ca^{2+}$-mediated activation of Rap1 in human platelets. *EMBO J.* **16,** 252–259.

Ghosh, P., Griffith, J., Geuze, H. J., and Kornfeld, S. (2003). Mammalian GGAs act together to sort mannose 6-phosphate receptors. *J. Cell Biol.* **163,** 755–766.

Ghosh, P., and Kornfeld, S. (2004). The GGA proteins: Key players in protein sorting at the *trans*-Golgi network. *Eur. J. Cell Biol.* **83,** 257–262.

Herrmann, C., Martin, G. A., and Wittinghofer, A. (1995). Quantitative-analysis of the complex between P21(Ras) and the Ras-binding domain of the human Raf-1 protein-kinase. *J. Biol. Chem.* **270,** 2901–2905.

Hirsch, D. S., Stanley, K. T., Chen, L. X., Jacques, K. M., Puertollano, R., and Randazzo, P. A. (2003). Arf regulates interaction of GGA with mannose-6-phosphate receptor. *Traffic* **4,** 26–35.

Hirst, J., Lui, W. W. Y., Bright, N. A., Totty, N., Seaman, M. N. J., and Robinson, M. S. (2000). A family of proteins with gamma-adaptin and VHS domains that facilitate trafficking between the *trans*-Golgi network and the vacuole/lysosome. *J. Cell Biol.* **149,** 67–79.

Jacques, K. M., Nie, Z. Z., Stauffer, S., Hirsch, D. S., Chen, L. X., Stanley, K. T., and Randazzo, P. A. (2002). Arf1 dissociates from the clathrin adaptor GGA prior to being inactivated by arf GTPase-activating proteins. *J. Biol. Chem.* **277,** 47235–47241.

Kirchhausen, T. (2002). Clathrin adaptors really adapt. *Cell* **109,** 413–416.

Kuai, J., Boman, A. L., Arnold, R. S., Zhu, X. J., and Kahn, R. A. (2000). Effects of activated ADP-ribosylation factors on Golgi morphology require neither activation of phospholipase D1 nor recruitment of coatomer. *J. Biol. Chem.* **275,** 4022–4032.

Kuai, J., and Kahn, R. A. (2000). Residues forming a hydrophobic pocket in ARF3 are determinants of GDP dissociation and effector interactions. *FEBS Lett.* **487,** 252–256.

Lui, W. W. Y., Collins, B. M., Hirst, J., Motley, A., Millar, C., Schu, P., Owen, D. J., and Robinson, M. S. (2003). Binding partners for the COOH-terminal appendage domains of the GGAs and gamma-adaptin. *Mol. Biol. Cell* **14,** 2385–2398.

Mattera, R., Arighi, C. N., Lodge, R., Zerial, M., and Bonifacino, J. S. (2003). Divalent interaction of the GGAs with the Rabaptin-5-Rabex-5 complex. *EMBO J.* **22,** 78–88.

Mattera, R., Puertollano, R., Smith, W. J., and Bonifacino, J. S. (2004). The trihelical bundle subdomain of the GGA proteins interacts with multiple partners through overlapping but distinct sites. *J. Biol. Chem.* **279,** 31409–31418.

Miller, G. J., Mattera, R., Bonifacino, J. S., and Hurley, J. H. (2003). Recognition of accessory protein motifs by the gamma-adaptin ear domain of GGA3. *Nat. Struct. Biol.* **10,** 599–606.

Misra, S., Puertollano, R., Bonifacino, J. S., and Hurley, J. H. (2001). Structural basis of acidic/dileucine-motif-based sorting by GGA proteins. *Mol. Biol. Cell* **12,** 85A.

Moss, J., and Vaughan, M. (1998). Molecules in the ARF orbit. *J. Biol. Chem.* **273,** 21431–21434.

Nakayama, K., and Wakatsuki, S. (2003). The structures and function of GGAs, the traffic controllers at the TGN sorting crossroads. *Cell Struct. Funct.* **28,** 431–442.

Nie, Z. Z., Hirsch, D. S., and Randazzo, P. A. (2003). Arf and its many interactors. *Curr. Opin. Cell Biol.* **15,** 396–404.

Nielsen, M. S., Madsen, P., Christensen, E. I., Nykjaer, A., Gliemann, J., Kasper, D., Pohlmann, R., and Petersen, C. M. (2001). The sortilin cytoplasmic tail conveys Golgi-endosome transport and binds the VHS domain of the GGA2 sorting protein. *EMBO J.* **20,** 2180–2190.

Nogi, T., Shiba, Y., Kawasaki, M., Shiba, T., Matsugaki, N., Igarashi, N., Suzuki, M., Kato, R., Takatsu, H., Nakayama, K., and Wakatsuki, S. (2002). Structural basis for the accessory protein recruitment by the gamma-adaptin ear domain. *Nat. Struct. Biol.* **9,** 527–531.

Owen, D. J., Collins, B. M., and Evans, P. R. (2004). Adaptors for clathrin coats: Structure and function. *Ann. Rev. Cell Dev. Biol.* **20,** 153–191.

Puertollano, R., Aguilar, R. C., Gorshkova, I., Crouch, R. J., and Bonifacino, J. S. (2001a). Sorting of mannose 6-phosphate receptors mediated by the GGAs. *Science* **292,** 1712–1716.

Puertollano, R., Randazzo, P. A., Presley, J. F., Hartnell, L. M., and Bonifacino, J. S. (2001b). The GGAs promote ARF-dependent recruitment of clathrin to the TGN. *Cell* **105,** 93–102.

Randazzo, P. A., Nie, Z., Miura, K., and Hsu, V. (2000). Molecular aspects of the cellular activities of ADP-ribosylation factors. *Sci. STKE* **59,** RE1.

Randazzo, P. A., Miura, K., and Jackson, T. R. (2001). Assay and purification of phosphoinositide-dependent ADP-ribosylation factor (ARF) GTPase activating proteins. *Methods Enzymol.* **329,** 343–354.

Robinson, M. S., and Bonifacino, J. S. (2001). Adaptor-related proteins. *Curr. Opin. Cell Biol.* **13,** 444–453.

Sander, E. E., van Delft, S., ten Klooster, J. P., Reid, T., van der Kammen, R. A., Michiels, F., and Collard, J. G. (1998). Matrix-dependent Tiam1/Rac signaling in epithelial cells promotes either cell-cell adhesion or cell migration and is regulated by phosphatidylinositol 3-kinase. *J. Cell Biol.* **143,** 1385–1398.

Santy, L. C., and Casanova, J. E. (2001). Activation of ARF6 by ARNO stimulates epithelial cell migration through downstream activation of both Rac1 and phospholipase D. *J. Cell Biol.* **154,** 599–610.

Scott, P. M., Bilodeau, P. S., Zhdankina, O., Winistorfer, S. C., Hauglund, M. J., Allaman, M. M., Kearney, W. R., Robertson, A. D., Boman, A. L., and Piper, R. C. (2004). GGA proteins bind ubiquitin to facilitate sorting at the *trans*-Golgi network. *Nat. Cell Biol.* **6,** 252–259.

Shiba, Y., Katoh, Y., Shiba, T., Yoshino, K., Takatsu, H., Kobayashi, H., Shin, H. W., Wakatsuki, S., and Nakayama, K. (2004). GAT (GGA and Tom1) domain responsible for ubiquitin binding and ubiquitination. *J. Biol. Chem.* **279,** 7105–7111.

Spang, A. (2002). Arf1 regulatory factors and COPI vesicle formation. *Curr. Opin. Cell Biol.* **14,** 423–427.

Springer, S., Spang, A., and Schekman, R. (1999). A primer on vesicle budding. *Cell* **97,** 145–148.

Takatsu, H., Katoh, Y., Shiba, Y., and Nakayama, K. (2001). Golgi-localizing, gammaadaptin ear homology domain, ADP-ribosylation factor-binding (GGA) proteins interact with acidic dileucine sequences within the cytoplasmic domains of sorting receptors through their Vps27p/Hrs/STAM (VHS) domains. *J. Biol. Chem.* **276,** 28541–28545.

Yoon, H.-Y., Jacques, K., Nealon, B., Stauffer, S., Premont, R. T., and Randazzo, P. A. (2004). Differences between AGAP1, ASAP1 and Arf GAP1 in substrate recognition: Interaction with the N-terminus of Arf1. *Cell. Signal.* **16,** 1033–1044.

Zhai, P., He, X. Y., Liu, J. A., Wakeham, N., Zhu, G. Y., Li, G. P., Tang, J., and Zhang, X. J. C. (2003). The interaction of the human GGA1 GAT domain with Rabaptin-5 is mediated by residues on its three-helix bundle. *Biochemistry* **42,** 13901–13908.

Zhu, G. Y., He, X. Y., Zhai, P., Terzyan, S., Tang, J., and Zhang, X. J. C. (2003a). Crystal structure of GGA2 VHS domain and its implication in plasticity in the ligand binding pocket. *FEBS Lett.* **537,** 171–176.

Zhu, G. Y., Zhai, P., He, X. Y., Terzyan, S., Zhang, R. G., Joachimiak, A., Tang, J., and Zhang, X. J. C. (2003b). Crystal structure of the human GGA1 GAT domain. *Biochemistry* **42,** 6392–6399.

Zhu, G. Y., Zhai, P., He, X. Y., Wakeham, N., Rodgers, K., Li, G. P., Tang, J., and Zhang, X. J. C. (2004). Crystal structure of human GGA1 GAT domain complexed with the GAT-binding domain of Rabaptin5. *EMBO J.* **23,** 3909–3917.

# [29] The Role of EFA6, Exchange Factor for Arf6, for Tight Junction Assembly, Functions, and Interaction with the Actin Cytoskeleton

*By* Frédéric Luton

## Abstract

In polarized epithelial cells, the tight junction has been ascribed several functions including the regulation of the paracellular permeability, an impediment to the diffusion of molecules between the apical and basolateral domains, a site of delivery of transport vesicles for basolateral proteins, and a scaffold for structural and signaling molecules. The tight junction is anchored physically into the apical actin cytoskeleton circumscribing the cell, which is known as the perijunctional actomyosin ring. This connection was first suggested by experiments using the actin depolymerizing drug cytochalasin, which was also found to disrupt the transepithelial permeability. Since then a large number of studies have reported the effects of drugs, molecular tools, or physiological and pathological conditions that alter coordinately actin organization and the tight junction. In support of this model, proteins of the tight junction, such as the members of

METHODS IN ENZYMOLOGY, VOL. 404 0076-6879/05 $35.00

DOI: 10.1016/S0076-6879(05)04029-2